Neuroscience 580 (2025) 383–393

Contents lists available at ScienceDirect

Neuroscience

journal homepage: www.elsevier.com/locate/nsc

Research Article

Task-state EEG feature extraction for spatial cognition analysis: a power spectral density and permutation conditional mutual information approach

Yijun Liu [a], Mohd Shafie bin Mustafa [b,*], M Iqbal bin Saripan [c], Muhammad Rezal bin Kamel Ariffin [b], Xianglong Wan [d], Xianling Dong [e], Xifa Lan [f], Dong Wen [d,*]

[a] *Institute for Mathematical Research, Universiti Putra Malaysia, Serdang, Malaysia*
[b] *Department of Mathematics and Statistics, Faculty of Science, Universiti Putra Malaysia, Serdang, Malaysia*
[c] *Department of Computer and Communication Systems Engineering, Faculty of Engineering, Universiti Putra Malaysia, Serdang, Malaysia*
[d] *School of Intelligence Science and Technology, University of Science and Technology Beijing, Beijing, China*
[e] *Heibei International Research Center of Medical Engineering, Chengde Medical University, Chengde, China*
[f] *Department of Neurology, First Hospital of Qinhuangdao, Qinhuangdao, China*

ARTICLE INFO

Keywords:
Spatial cognitive training
Virtual reality
Task-state EEG signals
Power spectral density permutation conditional mutual information

ABSTRACT

The permutation conditional mutual information (PCMI) method which combined time and spatial domain information was found effective in analyzing EEG signals of neuron groups. Considering the absence of frequency domain information in the PCMI algorithm, a feature extraction method based on Power Spectral Density Permutation Conditional Mutual Information (PSDPCMI) was first proposed to analyze task-state EEG signals. In this study, the performance of the PSDPCMI algorithm was employed for a VR spatial cognitive training experiment based on a Virtual Community training game and a Virtual City Walking testing game as carriers for subjects' training and evaluation. The PSD, PCMI, and PSDPLV feature extraction methods were compared with the proposed PSDPCMI algorithm. According to the results, the highest classification accuracy was achieved across all frequency bands, with notable performance in the Theta, Beta2, and Gamma frequency bands. Besides, the new algorithm proposed also had higher precision, recall, F1-score, and AUC-score than the PSD, PCMI, and PSDPLV algorithms in most frequency bands and performed well in the classification accuracy of different classification models and another spatial cognitive dataset. The experimental outcomes demonstrated that the proposed PSDPCMI method in feature extraction showed a significant performance for the EEG signal analysis.

Introduction

Task-state electroencephalogram (EEG) contains information related to the basis of brain activity and its network connectivity. According to recent research, task-state EEG can be used as an aid in diagnosing patients with cognitive impairment (Wen et al., 2022; Zhang et al., 2022). EEG signals are usually high-dimensional and large. In processing EEG signals, the feature extraction method is an important step. The feature extraction methods for EEG signals that have been widely used in recent years are based on Granger Causality Analysis (GCA) (Chen et al., 2021; Lin et al., 2024; Zhang et al., 2022), Power Spectral Density (Alam et al., 2020; Lai et al., 2019; Hasan et al., 2020), Independent Component Analysis (ICA) (Ramkumar and Paulraj, 2025; Rashida and Habib, 2024; White et al., 2012), Wavelet Transform (Ananthi et al., 2024; Dişli et al., 2025), and Mutual Information (Li and Ouyang, 2010; Hassan et al., 2022; Wen et al., 2023; Wen et al., 2016).

Mutual Information discusses the correlation degree of two pieces of information in joint entropy, and Conditional Mutual Information is mutual information where conditions occur. Apart from external interference, this condition can better reflect the degree of interdependence between two random variables independent of external conditions (Palus and Vejmelka, 2007). Later, when studying the direction of cardiopulmonary coupling, permutation analysis and conditional mutual information were combined for consideration, and this idea was introduced into the consideration of the coupling relationship between brain regions. Finally, Permutation Conditional Mutual Information (PCMI) was formed. Li et al. first applied the PCMI method to the analysis of EEG signals in focal epilepsy rats to evaluate the coupling direction between

* Corresponding authors.
E-mail addresses: mshafie@upm.edu.my (M.S. bin Mustafa), wencangdong@163.com (D. Wen).

https://doi.org/10.1016/j.neuroscience.2025.06.036
Received 8 December 2024; Accepted 17 June 2025
Available online 19 June 2025

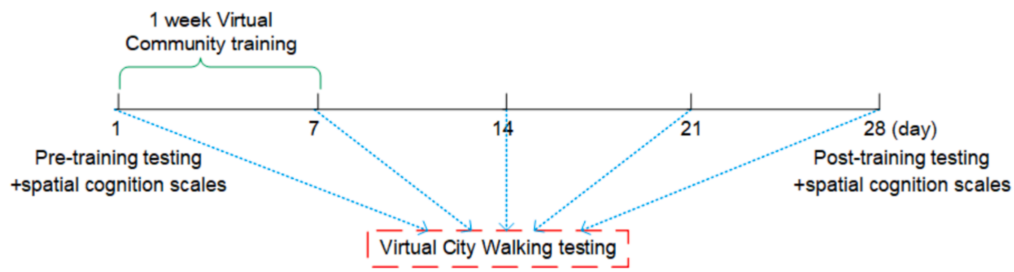

Fig. 1. Graphic description of the experiment.

Table 1
Statistical analysis of spatial cognitive scales before and after training.

Scale	Mean before training	Mean after training	T value	Degree of freedom	P value
CBTT	37.14 ± 16.48	50 ± 6.83	−2.463	6	0.049
GZSOT	4.86 ± 5.16	9.89 ± 6.20	−2.738	6	0.034
PTSOT	35.75 ± 9.81	19.32 ± 7.72	5.990	6	0.001

neuron populations (Li and Ouyang, 2010). The method was effective in analyzing EGG signals of neuron groups, and its performance was superior to the Conditional Mutual Information method and Granger Causality method. While PCMI proves effective in assessing coupling attributes across time and spatial domains, it falls short in incorporating information from the frequency domain. Relevant studies have shown that frequency domain information can improve the analysis performance of EEG signal time domain information (Chamanzar et al., 2017; Lv et al., 2022; Liu et al., 2016). Power Spectral Density (PSD) can make up for this disadvantage and extract characteristics in the frequency domain. In power spectral density analysis, the rhythm characteristics of EEG reflect the discharge law of cortical neuron groups, which reflects cortical function, and the different rhythm characteristics of different cortices reflect the complexity of brain activity (Alam et al., 2020; Lai et al., 2019; Hasan et al., 2020).

In the detection technology of mild cognitive decline based on EEG artificial intelligence, the existing research only extracted a certain feature of EEG signals or simply spliced multiple features (Ieracitano et al., 2020). While it has been proven that using fusion features can achieve higher accuracy than using only a certain set of features, this has led to these methods failing to take into account the correlation between features, leading to the size disaster problem. In 2022, Duan et al. proposed a PSDPLV feature extraction method by extracting the Power Spectral Density (PSD) and Phase Locking Value (PLV) features (Duan et al., 2022). They fused two features by matrix operation, and obtained high accuracy, showing the effectiveness of the fusion method.

Therefore, in this study, a time-spatial domain and frequency domain EEG fusion feature extraction method based on PSDPCMI was proposed. First, the PSD which indicated frequency domain information features and PCMI which indicated time-spatial information features were extracted and transformed, then the feature fusion was realized by matrix operation. For time-spatial domain characteristics, the PCMI method was used to characterize the predictability and regularity of the signals, thereby quantifying the complexity of the signals and representing the relationship between the cortex and cortical neural activity. For frequency domain characteristics, the PSD method was employed to describe the distribution characteristics of EEG power along frequency, which can visualize the distribution law of EEG rhythm (Wang, 2022). Many studies have shown that spatial cognitive training tasks can improve cognitive performance (Papakostas et al., 2021; Othman et al., 2022). The validity of the PSDPCMI fusion feature extraction method was verified based on spatial cognitive task-state EEG signals in this paper.

Material and methods

Data set

Data set description

This research used the same data set as the paper published by Wen et al. (2023). With the authorization of the Ethics Committee of Qinhuangdao First People's Hospital (Approval number: 2018B006), this experiment was conducted to assess the efficacy of a virtual community training game. A total of seven healthy people older than age 60 years were enrolled, all of whom joined the experiment's intervention group to engage with the virtual community game. According to the questionnaire survey, seven subjects had normal or corrected visual acuity, no color blindness, were right-handed, had no history of mental illness, had never participated in such spatial memory game training, and volunteered to participate in this study. The mean age of the participants was 67 ± 6.81 years, the male to female ratio was 2:5, and the mean education level was 10.5 ± 3.02 years.

All participants were given a 28-day spatial cognitive experiment in a quiet room. Over the 28 days, there was a mini-cycle every seven days, with six days of training and one day of testing for each mini-cycle. The experiment process was divided into three stages. And the graphic description of the experiment is shown in Fig. 1.

(1) Pre-training testing. Before the first phase of training, all subjects were evaluated with the CBTT (Kessels et al., 2000), GZSOT (Kyritsis and Gulliver, 2009), and PTSOT (Hegarty and Waller, 2004) spatial cognition scales and wore an OpenBCI EEG acquisition device and HTC Vive Focus headset VR glasses to carry out the Virtual City Walking (VCW) game to test their spatial cognition ability before training. Users were required to remember the reference buildings and routes along the way. Then, the original route was hidden, and the user was asked to retrace the learning route from memory.
(2) Training and phased testing. The experimental subjects used the Virtual Community VR game to carry out four weeks of training. Within this training game, a total of 16 virtual buildings were strategically positioned throughout the scene, aiding participants in establishing reference points for location determination. The participants first remembered the relative position of the target points and then searched for each target point according to the memory in the specified order. Among the training game, in order to ensure the enthusiasm of the subjects to participate, the experimental group was trained to use the "three-point goal" version of the virtual community in the first week and the "six-point goal" version of the virtual community in the last three weeks. And every other week, the experimental subjects used the Virtual City Walking (VCW) game for testing task.
(3) Post-training testing. At the end of the last phase, all subjects were tested with the Virtual City Walking testing game and spatial cognition scales. The results of EEG signals were archived to evaluate the effectiveness of training. Thus, the testing game

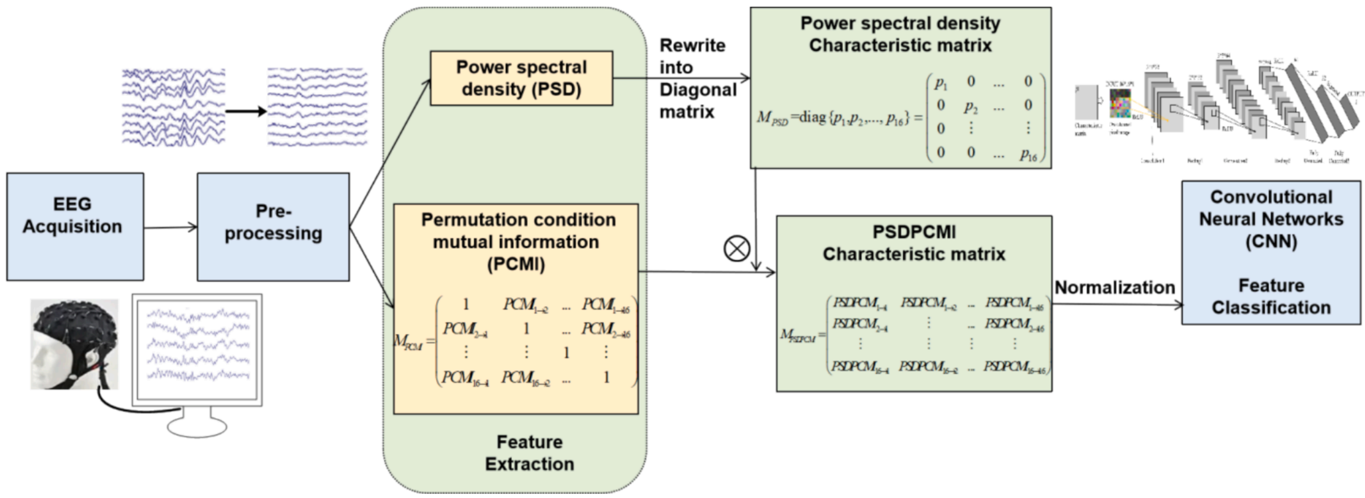

Fig. 2. Process of PSDPCMI fusion feature extraction method.

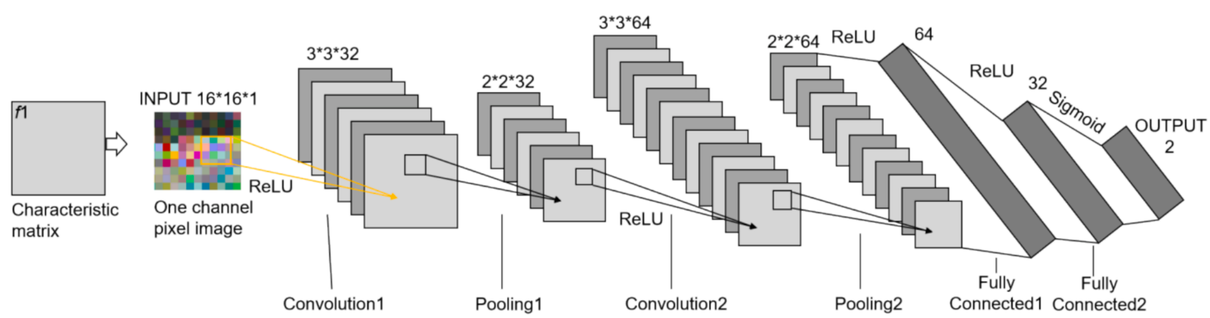

Fig. 3. Structure of CNN feature classification method.

was overall conducted five times. In order to keep the difficulty of each test consistent, each test route is symmetrized once.

As shown in Table 1, there were significant changes ($P < 0.05$) in the three spatial cognitive scales before and after training. The scores of CBTT and GZSOT scales were positively correlated with spatial cognitive ability and the scores of PTSOT scales were negatively correlated with spatial cognitive ability. The experimental subjects showed improved spatial cognitive ability after Virtual Community training. Thus, this task-state data set of testing game can be used to calculate the accuracy indexes of different feature extraction methods to distinguish the two states (before and after training).

Experimental data acquisition

During the process of the experiment, EEG signals from participants were collected using the OpenBCI EEG device. The device operated at a sampling rate of 125 Hz, with electrode impedance consistently maintained below 10 KΩ. For the purpose of synchronous acquisition of 16-channel EEG signals, two 8-channel Cyton amplifiers were employed. These amplifiers facilitated the transmission of data to the computer via a Bluetooth dongle jack.

Electrodes were placed according to the international standard lead 10–20 standard electrode placement method. Drawing upon extensive literature pertaining to spatial coding and retrieval using EEG signals (Bischof and Boulanger, 2003; Kober and Neuper, 2011; Sharma et al., 2017), a set of electrode positions was chosen as the requisite configuration for this experiment, adhered to commonly utilized standards. The sampling electrodes include: FP1, FP2, F7, F3, Fz, F4, F8, FCz, C3, Cz, C4, P7, Pz, P8, O1, O2, and sample reference electrodes A1 and A2 of the bilateral lobe mastoid process.

Preprocessing

In this study, Matlab toolbox EEGLAB and MNE-Python were used to preprocess the EEG signals. The following modules are included.

Step 1: Channel positioning. To ensure that Independent Component Analysis (ICA) can estimate the source location of independent components of data, the relative coordinate information of each channel needs to be imported.

Step 2: Bandpass filtering. The EEG signals were filtered using a filter of 1–50 Hz to remove high-frequency noise and low-frequency drift.

Step 3: Remove artifacts. To ensure a high signal-to-noise ratio, it is necessary to remove the motion artifacts, EOG and EMG, from EEG (Seok et al., 2021). In this study, the independent component analysis plug-in provided was used to calculate independent components and remove artifacts.

Step 4: Baseline correction. Usually, the data before 0 ms is taken as the baseline (Chen, 2016). Part of the spontaneous EEG noise could be eliminated by subtracting the average value of each point data before 0 ms from the data after 0 ms using EEGLAB.

Step 5: Extracting frequency band. In this research, the EEG signals were divided into seven frequency bands by MNE Python: Delta (1–4 Hz), Theta (4–8 Hz), Alpha1 (8–10.5 Hz), Alpha2 (10.5–13 Hz), Beta1 (13–20 Hz), Beta2 (20–30 Hz), and Gamma (30–50 Hz).

Step 6: Data segmentation. EEG epoch extraction was required. The pre-processed epochs were the EEG signals of the subjects one second before and one second after pressing the button in the testing game. The EEG data of subjects undergoing 5 minutes' VR testing was sliced with a 2-second window. Here, the waiting data in the early and late stages of the testing game was deleted.

Table 2
Classification results for PSD, PCMI, PSDPLV, and PSDPCMI methods of seven frequency bands.

(a) Delta frequency band

Method	Accuracy	Precision	Recall	F1-score	AUC-score
PSD	80.95 %	74.47 %	89.74 %	81.40 %	81.54 %
PCMI	90.48 %	92.11 %	87.5 %	89.74 %	90.34 %
PSDPLV	77.38 %	80.00 %	74.42 %	77.11 %	77.45 %
PSDPCMI	91.67 %	88.37 %	95.00 %	91.56 %	91.81 %

(b) Theta frequency band

Method	Accuracy	Precision	Recall	F1-score	AUC-score
PSD	76.19 %	67.31 %	92.11 %	77.78 %	77.57 %
PCMI	91.67 %	94.59 %	87.50 %	90.91 %	91.47 %
PSDPLV	86.90 %	85 %	87.18 %	86.08 %	86.92 %
PSDPCMI	95.24 %	97.37 %	92.50 %	94.87 %	95.11 %

(c) Alpha1 frequency band

Method	Accuracy	Precision	Recall	F1-score	AUC-score
PSD	77.38 %	68.52 %	94.87 %	79.57 %	78.55 %
PCMI	89.29 %	87.50 %	96.08 %	91.59 %	87.43 %
PSDPLV	82.14 %	80.49 %	82.50 %	81.48 %	82.16 %
PSDPCMI	94.05 %	92.68 %	95.00 %	93.83 %	94.09 %

(d) Alpha2 frequency band

Method	Accuracy	Precision	Recall	F1-score	AUC-score
PSD	70.24 %	61.29 %	97.44 %	75.25 %	72.05 %
PCMI	90.28 %	91.67 %	84.61 %	88.00 %	88.97 %
PSDPLV	83.33 %	79.55 %	87.50 %	83.33 %	83.52 %
PSDPCMI	94.05 %	93.75 %	90.91 %	92.31 %	93.49 %

(e) Beta1 frequency band

Method	Accuracy	Precision	Recall	F1-score	AUC-score
PSD	73.81 %	65.45 %	92.31 %	76.60 %	75.04 %
PCMI	91.67 %	94.44 %	87.18 %	90.67 %	91.37 %
PSDPLV	84.52 %	81.58 %	83.78 %	82.67 %	84.45 %
PSDPCMI	92.05 %	92.68 %	95.00 %	93.88 %	94.09 %

(f) Beta2 frequency band

Method	Accuracy	Precision	Recall	F1-score	AUC-score
PSD	76.19 %	67.27 %	94.87 %	78.72 %	77.44 %
PCMI	96.43 %	97.96 %	96.00 %	96.97 %	96.53 %
PSDPLV	94.05 %	95.35 %	93.18 %	94.25 %	94.09 %
PSDPCMI	96.43 %	93.62 %	99.98 %	96.70 %	96.25 %

(g) Gamma frequency band

Method	Accuracy	Precision	Recall	F1-score	AUC-score
PSD	79.76 %	69.81 %	97.37 %	81.32 %	81.29 %
PCMI	94.05 %	93.18 %	95.35 %	94.25 %	94.02 %
PSDPLV	92.86 %	91.30 %	95.45 %	93.33 %	91.48 %
PSDPCMI	96.43 %	97.44 %	95.00 %	96.20 %	96.36 %

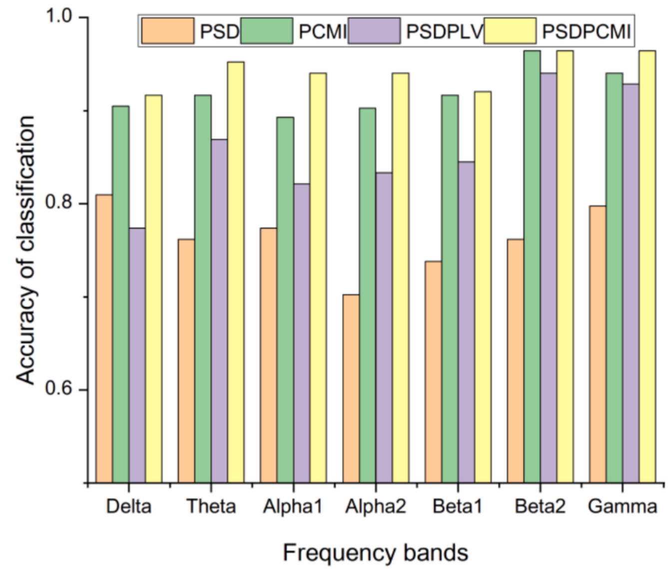

Fig. 4. Accuracy of classification for PSD, PCMI, PSDPLV, and PSDPCMI methods in seven frequency bands.

Related methods

Power spectral density (PSD)

PSD refers to the distribution of signal power at each frequency point with the concept of density. It is a measure of the mean square value of random variables and is the dimension of the average power per unit frequency. The PSD method mainly analyzes the change of signal energy with frequency, that is, the distribution of signal energy in the frequency domain.

In this paper, the Welch method was used to analyze the power spectrum energy of seven frequency bands. Welch method employed the average method to improve its variance characteristics and obtain the weighted overlapping average method, which was an improvement of the periodic graph method, also known as the Welch mean periodic graph method (Welch, 1967). Its principle is to divide the $x(n)$ data length N into L segments, calculate the power spectrum energy of each segment separately, and then average them. Each window can be hamming window, hanning window or rectangular window, and the window function $w(n)$ is selected as hanning window in this paper. According to Welch's method, the power spectrum of each window is denoted as $p_i(w)$, namely:

$$p_i(w) = \frac{1}{MU}\left|\sum_{n=0}^{M-1} x_i(n)w(n)e^{-jwn}\right|^2, i = 1, 2, ..., M-1 \quad (1)$$

where $M = N/L$ is each segment of data, which is also the window length. And U is the normalization factor, which is used to ensure that the obtained spectrum is a progressive unbiased estimate. Therefore, the average power spectrum obtained by Welch's average method is as follows.

$$p(w) = \frac{1}{MUL}\sum_{i=1}^{L}\left|\sum_{n=0}^{M-1} x_i(n)w(n)e^{-jwn}\right|^2 \quad (2)$$

This PSD method was used to extract seven frequency bands: Delta (1–4 Hz), Theta (4–8 Hz), Alpha1 (8–10.5 Hz), Alpha2 (10.5–13 Hz), Beta1 (13–20 Hz), Beta2 (20–30 Hz), Gamma (30–50 Hz) power spectrum features of all 16 electrodes in EEG signals. Different power spectrum density features can be extracted from the first and fifth testing of subjects. For the first and fifth testing data of each frequency band, the power spectral density of each electrode (16 electrodes) can be extracted, which is expressed as $PSD = \{p_1, p_2, ..., p_{16}\}$ in the form of a set, where p_i represents the power spectral density value corresponding to the ith electrode.

In the calculation of Power Spectral Density Permutation Conditional Mutual Information, the corresponding power of these 16 electrodes is rewritten into a matrix form. And the value of the power spectral density of these 16 electrodes is placed on the main diagonal of the matrix in accordance with the electrode number order, which is:

$$M_{PSD} = \mathrm{diag}\{p_1, p_2, ..., p_{16}\} = \begin{pmatrix} p_1 & 0 & \dots & 0 \\ 0 & p_2 & \dots & 0 \\ 0 & \vdots & & \vdots \\ 0 & 0 & \dots & p_{16} \end{pmatrix} \quad (3)$$

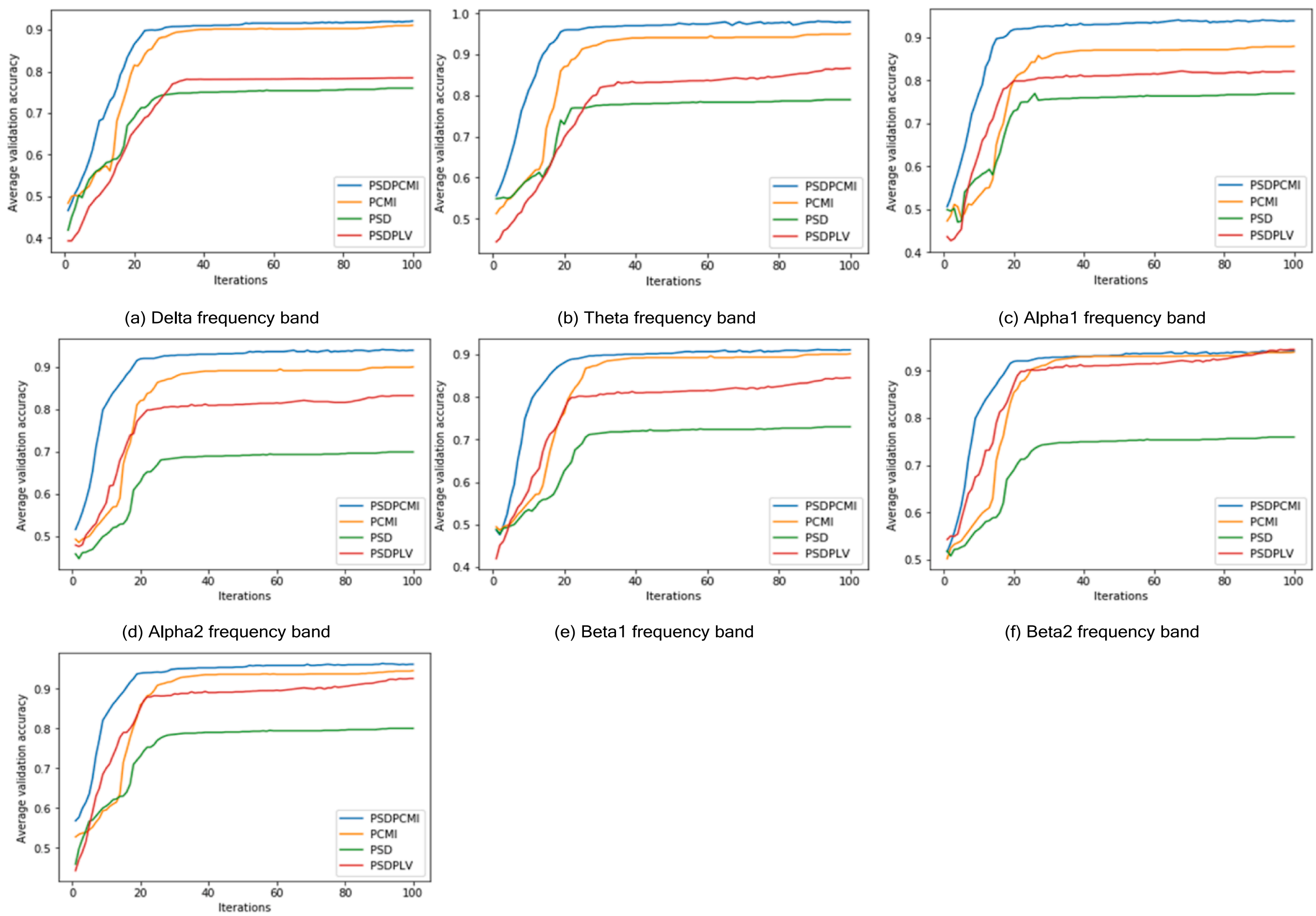

(a) Delta frequency band (b) Theta frequency band (c) Alpha1 frequency band

(d) Alpha2 frequency band (e) Beta1 frequency band (f) Beta2 frequency band

(g) Gamma frequency band

Fig. 5. Average validation accuracy curves of seven frequency bands.

Permutation conditional mutual information (PCMI)

In this study, PCMI was used to extract the time-spatial domain information from EEG data. Specifically, for EEG signals, the time series X and Y of two different EEG channels are selected, and the two sequences have the same length sampling points n. Vectors are extracted from X and Y time series at τ interval of time length, and the length of the vector is $m-$dimensional, so that the two time series can generate $n-(m-1)\tau$ new vectors, which are $X_i = (x_i, x_{i+\tau}, \ldots, x_{i+(m-1)\tau}), i = 1, \ldots, n-(m-1)\tau$ and $Y_j = \left(y_j, y_{j+\tau}, \ldots, y_{j+(m-1)\tau}\right), j = 1, \ldots, n-(m-1)\tau$.

The values of the $n-(m-1)\tau$ obtained space vectors are arranged in ascending order, and there could be $m!$ arrangement patterns according to the subscript results after the ordering of each space vector. The number of occurrences of each arrangement pattern $C_{\pi_i}, i = 1, 2, \ldots, m!$ and $C_{\pi_j}, j = 1, 2, \ldots, m!$ could be counted, and the probability are defined as:

$$P(X = \pi_i) = \frac{C_{\pi_i}}{n-(m-1)\tau}, i = 1, 2, \ldots, m! \tag{4}$$

$$P(Y = \pi_j) = \frac{C_{\pi_j}}{n-(m-1)\tau}, j = 1, 2, \ldots, m! \tag{5}$$

In this way, permutation entropy can be obtained, and there are $m! * m!$ joint permutation modes of two time series at the same time. Similarly, joint permutation entropy and conditional permutation entropy can be obtained; the calculation is shown as Eqs. (6)–(9).

$$PE(X) = -\sum_{i=1}^{m!} p(x_i)\log(p(x_i)) \tag{6}$$

$$PE(Y) = -\sum_{j=1}^{m!} p(y_j)\log(p(y_j)) \tag{7}$$

$$PE(X, Y) = -\sum_{i=1}^{m!}\sum_{j=1}^{m!} p(x_i, y_j)\log(p(x_i, y_j)) \tag{8}$$

$$PE(X|Y) = -\sum_{i=1}^{m!}\sum_{j=1}^{m!} p(x_i|y_j)\log(p(x_i|y_j)) \tag{9}$$

Permutation entropy can take the information content of time series with dynamic noise, in which the permutation mode has weak stationarity in the whole time series, which is exactly in line with the characteristics of EEG. According to Eq. (10), mutual information between EEG signals X and Y based on permutation mode can be obtained.

$$PMI(X;Y) = PE(X) + PE(Y) - PE(X, Y) \tag{10}$$

The condition in PCMI refers to the influence of the previous time series on the sequence at δ time in the future. Then $PE(X_\delta|X)$ is the conditional permutation entropy of X_δ under the existence of X. After introducing X_δ, PCMI can obtain at most $m! * m! * m!$ ordering modes, and there can also be joint permutation entropy and conditional joint permutation entropy.

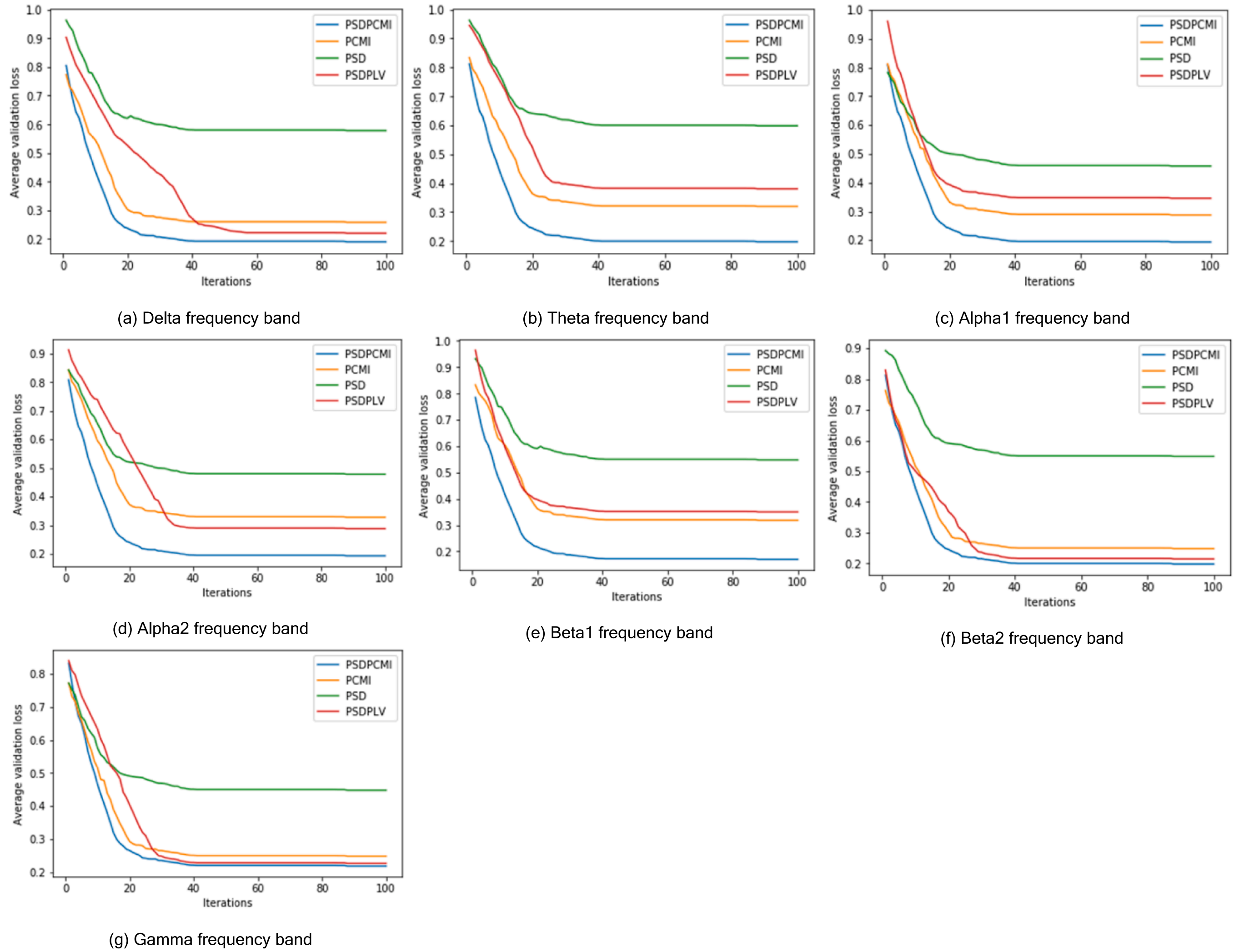

(a) Delta frequency band
(b) Theta frequency band
(c) Alpha1 frequency band
(d) Alpha2 frequency band
(e) Beta1 frequency band
(f) Beta2 frequency band
(g) Gamma frequency band

Fig. 6. Average validation loss curves of seven frequency bands.

$$PE(X,Y_\delta,Y) = -\sum_{i=1}^{m!}\sum_{j=1}^{m!}\sum_{k=1}^{m!}P(X=\pi_i,Y=\pi_j,Z=\pi_k)\log P(X=\pi_i,Y=\pi_j,Z=\pi_k) \tag{11}$$

$$PE(X,Y_\delta|Y) = PE(X,Y_\delta,Y)/PE(Y) \tag{12}$$

Finally, the permutation conditional mutual information of X to Y and Y to X of EEG signals can be obtained.

$$PCMI^\delta_{X\rightarrow Y} = PCMI(X;Y_\delta|Y) = PE(X|Y)+PE(Y_\delta|Y)-PE(X,Y_\delta|Y) \tag{13}$$

$$PCMI^\delta_{Y\rightarrow X} = PCMI(Y;X_\delta|X) = PE(Y|X)+PE(X_\delta|X)-PE(Y,X_\delta|X) \tag{14}$$

Since the delay time δ is uncertain, multiple numbers of δ are finally selected to get the average value.

$$PCMI_{X\rightarrow Y} = \frac{1}{N}\sum_{\delta=1}^{N}PCMI^\delta_{X\rightarrow Y} \tag{15}$$

$$PCMI_{Y\rightarrow X} = \frac{1}{N}\sum_{\delta=1}^{N}PCMI^\delta_{Y\rightarrow X} \tag{16}$$

where N refers to the maximum delay time, $PCMI_{X\rightarrow Y}$ represents the coupling strength from signal X to signal Y, $PCMI_{Y\rightarrow X}$ represents the coupling strength from signal Y to signal X.

In calculating PCMI, it is required to set the dimension of vector m, the maximum delay time N, and the interval time τ. According to the description of previous literature, the dimension m is set to 3, the maximum delay time N is set to 15, and the interval time τ is set to 11 (Wen, 2014).

The PCMI characteristic matrix of all 16 electrodes combinations can be represented by a matrix, as shown in Eq. (17),

$$M_{PCMI} = \begin{pmatrix} 1 & PCMI_{1\rightarrow 2} & \cdots & PCMI_{1\rightarrow 16} \\ PCMI_{2\rightarrow 1} & 1 & \cdots & PCMI_{2\rightarrow 16} \\ \vdots & \vdots & 1 & \vdots \\ PCMI_{16\rightarrow 1} & PCMI_{16\rightarrow 2} & \cdots & 1 \end{pmatrix} \tag{17}$$

where $PCMI_{i\rightarrow j}$ is the permutation conditional mutual information from electrode i to electrode j. Since the electrode's coupling strength to itself is 1, the diagonal elements of this matrix are all 1.

Power spectral density phase locking value (PSDPLV)

Duan et al. proposed a PSDPLV fusion feature extraction method in 2022, by extracting the EEG Power Spectral Density (PSD) and Phase Locking Value (PLV) brain network features (Duan et al., 2022). The two features were fused by matrix operation, and the fused features were classified by convolutional neural network. The method obtained high accuracy on the data set collected by a hospital in Shanghai. The results showed that the diagnostic accuracy of the PSDPLV brain network was better than that of the COH (coherence) and PLV brain network, PSD

Table 3
Classification accuracy for PSD, PCMI, PSDPLV, PSDPCMI methods under CNN, ELM and SVM methods of seven frequency bands.

(a) Delta frequency band

Method	PSD	PCMI	PSDPLV	PSDPCMI
CNN	80.95 %	90.48 %	77.38 %	91.67 %
ELM	84.52 %	85.71 %	69.05 %	86.90 %
SVM	78.57 %	92.86 %	58.33 %	85.71 %

(b) Theta frequency band

Method	**PSD**	**PCMI**	**PSDPLV**	**PSDPCMI**
CNN	76.19 %	91.67 %	86.90 %	95.24 %
ELM	90.48 %	85.71 %	69.05 %	92.86 %
SVM	77.38 %	90.48 %	55.95 %	91.67 %

(c) Alpha1 frequency band

Method	**PSD**	**PCMI**	**PSDPLV**	**PSDPCMI**
CNN	77.38 %	89.29 %	82.14 %	94.05 %
ELM	84.52 %	79.76 %	66.67 %	86.90 %
SVM	76.19 %	85.71 %	61.90 %	88.10 %

(d) Alpha2 frequency band

Method	**PSD**	**PCMI**	**PSDPLV**	**PSDPCMI**
CNN	70.24 %	90.28 %	83.33 %	94.05 %
ELM	85.71 %	78.57 %	72.62 %	85.71 %
SVM	71.43 %	79.76 %	63.10 %	86.90 %

(e) Beta1 frequency band

Method	**PSD**	**PCMI**	**PSDPLV**	**PSDPCMI**
CNN	73.81 %	91.67 %	84.52 %	92.05 %
ELM	88.10 %	86.90 %	73.81 %	94.05 %
SVM	82.14 %	94.05 %	65.48 %	96.43 %

(f) Beta2 frequency band

Method	**PSD**	**PCMI**	**PSDPLV**	**PSDPCMI**
CNN	76.19 %	96.43 %	94.05 %	96.43 %
ELM	91.67 %	91.67 %	77.38 %	96.43 %
SVM	85.71 %	94.05 %	72.62 %	95.24 %

(g) Gamma frequency band

Method	**PSD**	**PCMI**	**PSDPLV**	**PSDPCMI**
CNN	79.76 %	94.05 %	92.86 %	96.43 %
ELM	88.10 %	94.05 %	89.29 %	94.05 %
SVM	88.10 %	97.62 %	91.67 %	96.43 %

method, and PSDCOH brain network.

Following are the steps for calculating PLV for each electrode. First, obtain the phase $\Phi_x(t)$ and $\Phi_y(t)$ of the two signals $x(t)$ and $y(t)$ to compute phase difference $\Delta\Phi(t)$. Then, convert the phase difference into a complex number $e^{i\Delta\phi(t)}$ and calculate the mean of these complex numbers over time. In Eq. (19), N is the length of the time point, and the value of PLV ranges from 0 to 1. The PLV characteristic matrix of all 16 electrodes combinations can be calculated.

$$\Delta\Phi(t) = \Phi_x(t) - \Phi_y(t) \tag{18}$$

$$PLV = |\frac{1}{N}\sum_{n=1}^{N} e^{i(\Phi_1(n)-\Phi_2(n))}| \tag{19}$$

Power spectral density permutation conditional mutual information (PSDPCMI)

Following the design idea of PSDPLV, this paper proposed a new fusion method PSDPCMI based on PSD and PCMI. The overall process of PSDPCMI fusion feature extraction method is illustrated in Fig. 2. The method consists of the following steps: (1) EEG signal collection; (2) preprocess all the EEG data and divide the data into seven frequency bands; (3) extract the PSD features and PCMI features of all preprocessed EEG data; (4) rewrite the PSD features into the form of diagonal matrix, and perform the matrix multiplication with the PCMI features to obtain the PSDPCMI feature matrices; and (5) normalize the PSDPCMI feature matrices and put them into the Convolutional Neural Network (CNN) for classification. The PSDPLV matrix can also be calculated for subsequent comparisons by using PLV matrix instead of PCMI matrix.

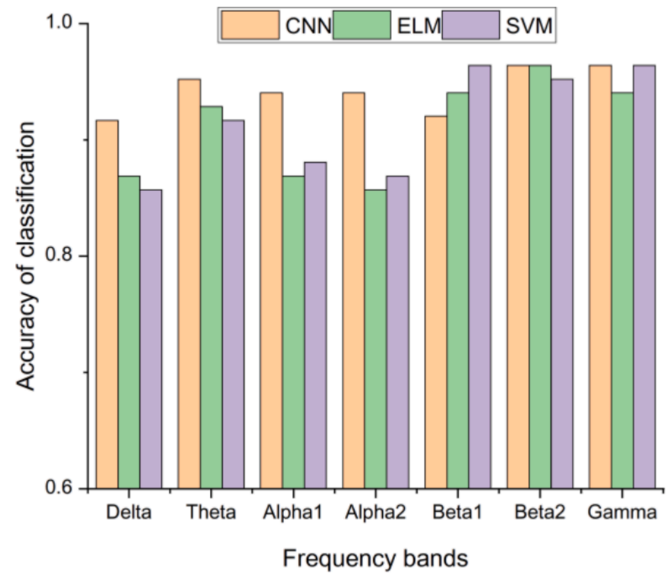

Fig. 7. Classification accuracy for PSDPCMI methods under CNN, ELM and SVM methods of seven frequency bands.

Classification and statistical analysis method

Convolutional Neural Network (CNN) is a kind of feed-forward neural network and one of the representative algorithms of deep learning. In recent years, many researchers have applied it to the data analysis of EEG signals and obtained good classification results (Mammone et al., 2020; Mao et al., 2020; Dai et al., 2020). The CNN network structure in this study is shown in Fig. 3.

The two-dimensional feature matrix obtained by the fusion feature combination method is taken as the input layer of the CNN model, and the dimension is 16*16*1. The second and fourth layers are the convolution layers. For the two-dimensional eigenmatrix of the input layer, 32 filters with a size of 3*3 and 64 filters with a size of 3*3, a moving step of 1 are used for convolution operation, and the activation function is Rectified Linear Unit (ReLU). The third and fifth layers select the maximum pooling layer with a size of 2*2 and a moving step of 1. The pooling layer realizes a dimensionality reduction operation on the output matrix data of the previous layer. The sixth and seventh layers are fully connected layers, which contain 64 and 32 neurons respectively, and are nonlinearly transformed by ReLU activation function. The final layer, the output layer, contains 2 neurons and uses the Sigmoid activation function to achieve binary classification.

In the computation, 5-fold cross-validation was performed using the cross_val_score function in the sklearn library. In 5-fold cross-validation, the EEG data of all subjects were divided into 5 parts, including four training sets and one testing set. And took turns to select different parts of the five parts as the training set and testing set followed the rule of 5-fold cross-validation method. Finally, the average accuracy, precision,

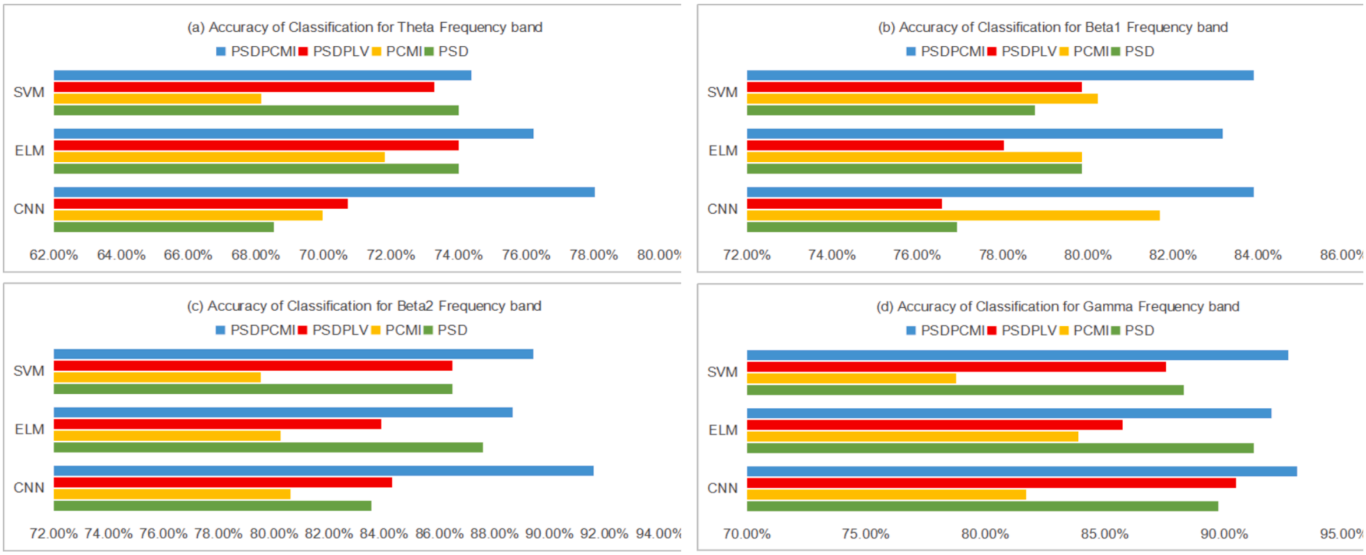

Fig. 8. Classification accuracy for PSD, PCMI, PSDPLV, and PSDPCMI methods under CNN, ELM and SVM methods of Theta, Beta 1, Beta 2, and Gamma frequency bands.

recall, F1-score, and AUC-score of all the results were used as performance indicators for the methods.

Results

Classification results for different feature extraction methods

In this paper, the attribute characteristics under PSD, PCMI, PSDPLV, and PSDPCMI methods of seven frequency bands were classified using CNN model for comparison. In Table 2(a)–(g), the proposed PSDPCMI presents the highest accuracy in seven frequency bands, the highest precision in Theta, Alpha1, Alpha2, and Gamma frequency bands, the highest recall in Delta, Theta, Beta1, and Beta2 frequency bands, and the highest F1-score and AUC-score in six frequency bands except Beta2 frequency band.

The PCMI method has the highest precision in Delta, Beta1, and Beta2 frequency bands, the highest recall in Alpha1 frequency band, the highest F1-score, and AUC-score in Beta2 frequency band. The PSDPLV fusion feature extraction method shows the highest recall in Gamma frequency band and the PSD method shows the highest recall in Alpha2 frequency band. Therefore, in general, the PSDPCMI feature fusion method is superior to the other three methods in feature extraction.

Fig. 4 illustrates the accuracy of the PSD, PCMI, PSDLPV, and PSDPCMI methods in seven frequency bands. From the graph, it can be seen that the PSDPCMI algorithm has the highest accuracy in seven frequency bands. The PCMI algorithm has the second highest accuracy. The PSDPLV method ranks third in accuracy. The PSD algorithm has the lowest accuracy. Moreover, among the results of seven frequency bands, Theta, Beta2, and Gamma frequency bands have the highest accuracy under the PSDPCMI method, which shows these three frequency bands maybe more sensitive to the VR spatial cognitive training.

Average validation accuracy and loss curves for different feature extraction methods

Average validation accuracy curves for different feature extraction methods

Fig. 5(a)–(g) shows the average validation accuracy curves of seven frequency bands for four methods. Among them, the curves of PSDPCMI feature set increase the fastest, and the validation accuracy of PSDPCMI feature set is higher than that of PSD, PCMI, and PSDPLV feature sets. The average validation accuracy curves of PSDPCMI method tend to be stable after 20 iterations in seven frequency bands. In addition, the average validation accuracy values of PSDPCMI reach near 0.95.

Average validation loss curves for different feature extraction methods

Fig. 6(a)–(g) shows the average validation loss curves of seven frequency bands for four methods. The average validation loss curves of PSDPCMI feature set decrease the fastest, and the loss values of PSDPCMI feature set are lower than those of PSD, PCMI, and PSDPLV feature sets when they become stable, and the loss values are the smallest which is less than 0.2. The average validation loss curves of the four methods tend to be stable after 40 iterations.

Comparison of classification performance for different feature classification methods

In this section, Extreme Learning Machines (ELM), Support Vector Machines (SVM), and Convolutional Neural Network (CNN) were applied to the features extracted by PSD, PCMI, PSDPLV, and PSDPCMI methods for classification. For the CNN feature classification method, the structure of method is shown in Fig. 3. For the SVM and ELM feature classification methods, the optimal parameter combinations and hidden_units were respectively searched in seven frequency bands. The classification accuracy results are shown in Table3(a)-(g). For the PSDPCMI method, the CNN classifier has the highest classification accuracy in six frequency bands except Beta1 frequency band. It can be seen that among the three classical classifiers, CNN and PSDPCMI proposed in this paper have the best fit.

Fig. 7 compares the classification accuracy for PSDPCMI method under different classifiers of seven frequency bands. The proposed PSDPCMI method performs well for the classification accuracy of the three classifiers, and the classification accuracy is all greater than 85 %. For Theta, Beta 1, Beta2, and Gamma frequency bands, the classification accuracy of the three classifiers is even higher than 91 %. To sum up, different classifiers were used to classify PSDPCMI characteristics in this research. From the classification results of the evaluation indexes, the influence of the three classifiers on the classification results was small.

Method validation in spatial cognitive dataset

Another spatial cognitive data set method validation was also used for PSDPCMI method feature extraction validation. In this dataset, a total of 16 university students were recruited to participate in the group spatial cognitive training experiment at the University of Science and

Technology Beijing (Approval number: 2022-1-104). The 16 subjects were divided into four groups for 28 days, and the training was based on the group VR racing game. During the training period, the Virtual City Walking testing game was conducted every other week. The EEG data during the testing game was recorded and preprocessed as the previous data set. According to the comparison of the subjects' CBTT, GZSOT, and PTSOT spatial cognition scales before and after training, it was found that the subjects' spatial cognition ability was significantly improved after training ($P < 0.05$). Here, this task-state spatial cognitive data set was used to calculate the accuracy of classification of different feature extraction methods for different classification models to distinguish the two states (before and after training). This dataset applied the same hyperparameters in CNN feature classification as normal healthy people older than age 60 years dataset in seven frequency bands, as shown in Fig. 3. And for SVM and ELM feature classification methods, the optimal parameter combinations and hidden_units were respectively searched in seven frequency bands.

In Fig. 8, four feature extraction methods, PSD, PCMI, PSDPLV, and PSDPCMI, were used in the new data set, and then CNN, ELM, and SVM were used for feature classification. Here, only four of the seven frequency band results with the higher average accuracy are selected for display, which are Theta, Beta 1, Beta 2, and Gamma frequency bands as shown in Fig. 8. Clearly, the high classification accuracy results of Theta, Beta2, and Gamma frequency bands under PSDPCMI and CNN methods are consistent with the results of the previous dataset. The classification accuracy of Beta 2 and Gamma frequency bands under PSDPCMI and CNN methods is even higher, which is more than 91.5 %. It can also be seen from the results that using PSDPCMI for feature extraction and CNN for feature classification has the best classification accuracy in the four frequency bands. This dataset verified the validity of PSDPCMI feature extraction method and its good matching with CNN classifier.

Discussion

Feasibility and effectiveness of PSDPCMI method

In the field of electroencephalography, power spectral density (PSD) can provide useful information about the frequency characteristics of brain activity (Alam et al., 2020; Lai et al., 2019; Hasan et al., 2020). But PSD has the problem of insufficient expression of time and spatial domain features (Hasan et al., 2020). Permutation Conditional Mutual Information (PCMI) is proposed to study the coupling relationship between neural signals and validate its effectiveness in extracting the coupling features of neural data (Wen et al., 2016; Cui et al., 2016). It has been proven that the feature extraction method has better classification accuracy than Conditional Mutual Information method and Granger Causality Analysis (Li and Ouyang, 2010). In addition, simulations have shown that the PCMI method is superior to the transfer entropy and causal entropy methods at identifying the coupling direction between the spike trains (Li et al., 2011). However, PCMI only analyzes the coupling characteristics in the time and spatial domains, without considering the information in the frequency domain. Relevant studies showed that frequency domain information could improve the performance of EEG signal analysis in time domain (Chamanzar et al., 2017; Lv et al., 2022; Liu et al., 2016).

Thus, in this method, the PSD features which stand for frequency domain information were rewritten into the form of a diagonal matrix. The matrix multiplication was then performed with the PCMI features, which stand for the time-spatial domain information to obtain the PSDPCMI feature matrices. The classification results showed that the classification accuracy of PSDPCMI proposed in this study exceeded that of the PSD, PCMI, and PSDPLV methods in seven frequency bands. Although the average classification accuracy of PSDPCMI is 1 %–2 % lower than the results of the same data set by permutation conditional mutual information common space model (PCMICSP), which extracts the features of five frequency bands combination, the computational effort is greatly reduced (Wen et al., 2023).

The advantages of the PSDPCMI feature fusion method proposed in this paper are as follows. (1) Each element in the PSDPCMI feature matrix is calculated by multiplying the permutation conditional mutual information of the corresponding electrode's power spectral density. Therefore, each one-dimensional feature comprehensively considers the mutual information of power spectral density and ordering conditions, which is not available in simple feature splicing. Besides, this operation does not increase the number of features, which is beneficial for small sample classification; and (2) due to the difference in the value of power spectral density between different electrodes, the multiplication of PSD diagonal matrix and PCMI characteristic matrix can better highlight the correlation between the electrodes with larger power. Then slightly ignore the electrodes with smaller energy, which in essence can better highlight important features.

Clinical performance of PSDPCMI method

Although there are only seven subjects in this paper; therefore, the sample size is not large, but the robustness of the sample has been tested in the previous paper (Wen et al., 2023). Based on the results in this paper, the PSDPCMI method is more effective than PSD, PCMI, and PSDPLV in high and low cognitive abilities' classification. This result is also consistent with the inference of PSDPCMI method. From previous literatures, the PCMI method and its modified methods had good feature extraction effects in the cognitive field, especially in the spatial cognitive field (Wan et al., 2025; Wen et al., 2023). Therefore, it can be inferred that PSDPCMI features are also related to spatial cognition training.

In the average validation accuracy curves, the curve of PSDPCMI feature set rises faster than the other three methods, reaching the highest accuracy. In the average validation loss curves, the curve of PSDPCMI feature set decreases the fastest, obtaining the lowest loss value. Moreover, the results indicate that the classification of PSDPCMI features is the best, with the average classification accuracy of the seven frequency bands being more than 94 %, and the influence of different classifiers on the classification results is small. PSDPCMI continues to perform well on another spatial cognitive training dataset, especially in the Beta2 and Gamma frequency bands, proving that the proposed algorithm has better clinical application performance than previous algorithms.

The top three classification accuracy frequency bands are Theta, Beta2, and Gamma for PSDPCMI method under CNN classifier. The results are similar to those of previous studies; the changes in the Theta and Gamma frequency bands are positively correlated with more efficient navigation performance (White et al., 2012). Neurofeedback training targeting Beta frequency band can improve performance on cognitive tasks, especially those requiring sustained attention or working memory (Rogala et al., 2016). Calculations involving the Gamma band can more accurately distinguish between high and low cognitive abilities (Başar et al., 2019). Combing the classification accuracy of the second data set, the PSDPCMI characteristics in the Beta2 and Gamma frequency bands may also be an effective biomarker for high and low spatial cognitive abilities.

Since the sample size of this paper is limited, a deep learning model with more hidden layers cannot be employed for the CNN model. Perhaps the method can be further verified by adding more EEG signal samples in the future. In addition, for future development direction, a classifier that best matches the feature extraction method might be chosen to compare with the CNN method to improve classification performance.

Conclusion

In this research, a feature fusion extraction method for EEG signals based on the PSD and PCMI methods was proposed. This PSDPCMI method combined frequency domain and time-spatial domain to analyze the EEG signals. And its classification performance was better than the

PSD and PCMI feature extraction methods, as well as the recently proposed PSDPLV method. The experimental outcomes demonstrated the suitability of proposed method for feature extraction of spatial cognitive EEG signals in the classification of high and low cognitive abilities. However, the feature fusion method proposed in this paper is relatively complex and requires a certain amount of computation. Moving forward, we will continue to focus on and improve feature extraction and feature fusion methods to extract more EEG features to automatically diagnose cognitive decline.

CRediT authorship contribution statement

Yijun Liu: Writing – original draft, Visualization, Validation, Software, Methodology, Investigation, Conceptualization. **Mohd Shafie bin Mustafa:** Writing – review & editing, Supervision, Methodology, Conceptualization. **M Iqbal bin Saripan:** Writing – review & editing, Supervision. **Muhammad Rezal bin Kamel Ariffin:** Writing – review & editing, Supervision. **Xianglong Wan:** Writing – review & editing, Supervision. **Xianling Dong:** Writing – review & editing, Supervision. **Xifa Lan:** Investigation. **Dong Wen:** Writing – review & editing, Supervision, Methodology, Investigation, Funding acquisition, Conceptualization.

Declaration of competing interest

The authors declare that they have no known competing financial interests or personal relationships that could have appeared to influence the work reported in this paper.

Acknowledgment

This research was funded by National Key Research and Development Program of China (2023YFF1203702), National Natural Science Foundation of China (62276022, 62206014).

References

Alam, R.U., Zhao, H., Goodwin, A., Kavehei, O., McEwan, A., 2020. Differences in power spectral densities and phase quantities due to processing of EEG signals. Sensors 20 (21), 6285. https://doi.org/10.3390/s20216285.

Ananthi, A., Subathra, M.S.P., George, S.T., Sairamya, N.J., 2024. Entropy-based feature extraction for classification of EEG signal using Lifting Wavelet Transform. Prz. Elektrotechniczny 100, 146–150.

Başar, M.D., Duru, A.D., Akan, A., 2019. Investigation of emotional changes using features of EEG-Gamma band and different classifiers. In 2019 Medical Technologies Congress (TIPTEKNO). IEEE, pp. 1–4, Doi: 10.1109/TIPTEKNO.2019.8895088.

Bischof, W.F., Boulanger, P., 2003. Spatial navigation in virtual reality environments: an EEG analysis. Cyberpsychol. Behav. 6 (5), 487–495. https://doi.org/10.1089/109493103769710514.

Chamanzar, A., Shabany, M., Malekmohammadi, A., Mohammadinejad, S., 2017. Efficient hardware implementation of real-time low-power movement intention detector system using FFT and adaptive wavelet transform. IEEE Trans. Biomed. Circuits Syst. 11 (3), 585–596. https://doi.org/10.1109/TBCAS.2017.2669911.

Chen, J., 2016. Study on brain network connection characteristics and core nodes of AD patients based on resting state EEG. Tianjin Medical University. Master thesis.

Chen, D., Miao, R., Deng, Z., Han, N., Deng, C., 2021. Sparse granger causality analysis model based on sensors correlation for emotion recognition classification in electroencephalography. Front. Comput. Neurosci. 15, 684373. https://doi.org/10.3389/fncom.2021.684373.

Cui, D., Pu, W., Liu, J., Bian, Z., Li, Q., Wang, L., Gu, G., 2016. A new EEG synchronization strength analysis method: S-estimator based normalized weighted-permutation mutual information. Neural Netw. 82, 30–38. https://doi.org/10.1016/j.neunet.2016.06.008.

Dai, G., Zhou, J., Huang, J., Wang, N., 2020. HS-CNN: a CNN with hybrid convolution scale for EEG motor imagery classification. J. Neural Eng. 17 (1), 016025. https://doi.org/10.1088/1741-2552/ab5c91.

Dişli, F., Gedikpınar, M., Fırat, H., Şengür, A., Güldemir, H., Koundal, D., 2025. Epilepsy diagnosis from EEG Signals using continuous wavelet transform-based depthwise convolutional neural network model. Diagnostics 15 (1), 84. https://doi.org/10.3390/diagnostics15010084.

Duan, Z., Zhao, B., Li, C., 2022. Automatic detection of resting state EEG data for mild cognitive decline based on feature fusion method. Appl. Res. Computers/jisuanji Yingyong Yanjiu 39, 4. https://doi.org/10.19734/j.issn.1001-3695.2021.09.0417.

Hassan, K.M., Islam, M.R., Nguyen, T.T., Molla, M.K.I., 2022. Epileptic seizure detection in EEG using mutual information-based best individual feature selection. Expert Syst. Appl. 193, 116414. https://doi.org/10.1016/j.eswa.2022.116414.

Hasan, M.J., Shon, D., Im, K., Choi, H.K., Yoo, D.S., Kim, J.M., 2020. Sleep state classification using power spectral density and residual neural network with multichannel EEG signals. Appl. Sci. 10 (21), 7639. https://doi.org/10.3390/app10217639.

Hegarty, M., Waller, D., 2004. A dissociation between mental rotation and perspective-taking spatial abilities. Intelligence 32 (2), 175–191. https://doi.org/10.1016/j.intell.2003.12.001.

Ieracitano, C., Mammone, N., Hussain, A., Morabito, F.C., 2020. A novel multi-modal machine learning based approach for automatic classification of EEG recordings in dementia. Neural Netw. 123, 176–190. https://doi.org/10.1016/j.neunet.2019.12.006.

Kessels, R.P., Van Zandvoort, M.J., Postma, A., Kappelle, L.J., De Haan, E.H., 2000. The Corsi block-tapping task: standardization and normative data. Appl. Neuropsychol. 7 (4), 252–258. https://doi.org/10.1207/S15324826AN0704_8.

Kober, S.E., Neuper, C., 2011. Sex differences in human EEG theta oscillations during spatial navigation in virtual reality. Int. J. Psychophysiol. 79 (3), 347–355. https://doi.org/10.1016/j.ijpsycho.2010.12.002.

Kyritsis, M., Gulliver, S. R., 2009. Gilford Zimmerman orientation survey: A validation. In 2009 7th International Conference on Information, Communications and Signal Processing (ICICS). IEEE, pp. 1–4. Doi: 10.1109/ICICS.2009.5397592.

Lai, D., Heyat, M.B.B., Khan, F.I., Zhang, Y., 2019. Prognosis of sleep bruxism using power spectral density approach applied on EEG signal of both EMG1-EMG2 and ECG1-ECG2 channels. IEEE Access 7, 82553–82562. https://doi.org/10.1109/ACCESS.2019.2924181.

Li, X., Ouyang, G., 2010. Estimating coupling direction between neuronal populations with permutation conditional mutual information. Neuroimage 52 (2), 497–507. https://doi.org/10.1016/j.neuroimage.2010.05.003.

Li, Z., Ouyang, G., Li, D., Li, X., 2011. Characterization of the causality between spike trains with permutation conditional mutual information. Phys. Rev.—Statistical, Nonlinear, and Soft Matter Physics 84 (2), 021929. https://doi.org/10.1103/PhysRevE.84.021929.

Lin, R., Dong, C., Zhou, P., Ma, P., Ma, S., Chen, X., Liu, H., 2024. Motor imagery EEG task recognition using a nonlinear Granger causality feature extraction and an improved Salp swarm feature selection. Biomed. Signal Process. Control 88, 105626. https://doi.org/10.1016/j.bspc.2023.105626.

Liu, Z., Sun, J., Zhang, Y., Rolfe, P., 2016. Sleep staging from the EEG signal using multi-domain feature extraction. Biomed. Signal Process. Control 30, 86–97. https://doi.org/10.1016/j.bspc.2016.06.006.

Lv, Z., Zhang, J., Epota Oma, E., 2022. A Novel Method of Emotion Recognition from Multi-Band EEG Topology Maps based on ERENet. Appl. Sci. 12 (20), 10273. https://doi.org/10.3390/app122010273.

Mammone, N., Ieracitano, C., Morabito, F.C., 2020. A deep CNN approach to decode motor preparation of upper limbs from time–frequency maps of EEG signals at source level. Neural Netw. 124, 357–372. https://doi.org/10.1016/j.neunet.2020.01.027.

Mao, W.L., Fathurrahman, H.I.K., Lee, Y., Chang, T.W., 2020. EEG dataset classification using CNN method. In Journal of physics: conference series (Vol. 1456, No. 1, p. 012017). IOP Publishing. Doi: 10.1088/1742-6596/1456/1/012017.

Othman, M.Z., Hassan, Z., Has, A.T.C., 2022. Morris water maze: a versatile and pertinent tool for assessing spatial learning and memory. Exp. Anim. 71 (3), 264–280. https://doi.org/10.1538/expanim.21-0120.

Palus, M., Vejmelka, M., 2007. Directionality of coupling from bivariate time series: how to avoid false causalities and missed connections. Phys. Rev. E 75 (5), 056211. https://doi.org/10.1103/PhysRevE.75.056211.

Papakostas, C., Troussas, C., Krouska, A., Sgouropoulou, C., 2021. Exploration of augmented reality in spatial abilities training: a systematic literature review for the last decade. Inform. Educ. 20 (1), 107–130.

Ramkumar, E., Paulraj, M., 2025. Optimized FFNN with multichannel CSP-ICA framework of EEG signal for BCI. Comput. Methods Biomech. Biomed. Eng. 28 (1), 61–78. https://doi.org/10.1080/10255842.2024.2319701.

Rashida, M., Habib, M.A., 2024. Feature Extraction from Regenerated EEG–A better approach for ICA based eye blink artifact detection. Front. Biomed. Technolo. 11 (2), 199–206. https://doi.org/10.18502/fbt.v11i2.15336.

Rogala, J., Jurewicz, K., Paluch, K., Kublik, E., Cetnarski, R., Wróbel, A., 2016. The do's and don'ts of neurofeedback training: a review of the controlled studies using healthy adults. Front. Hum. Neurosci. 10, 301. https://doi.org/10.3389/fnhum.2016.00301.

Seok, D., Lee, S., Kim, M., Cho, J., Kim, C., 2021. Motion artifact removal techniques for wearable EEG and PPG sensor systems. Front. Electron. 2, 685513. https://doi.org/10.3389/felec.2021.685513.

Sharma, G., Gramann, K., Chandra, S., Singh, V., Mittal, A.P., 2017. Brain connectivity during encoding and retrieval of spatial information: individual differences in navigation skills. Brain Inf. 4, 207–217. https://doi.org/10.1007/s40708-017-0066-6.

Wan, X., Sun, Y., Wu, Z., Wen, D., 2025. Characterization of spatial cognitive EEG signals using normalized adjusted permutation conditional mutual information. Symmetry 17 (1), 130. https://doi.org/10.3390/sym17010130.

Wang Y., 2022. Study on time-frequence-space feature extraction and evaluation of resting EEG and TMS-EEG in consciousness disorders, PHD thesis.Yanshan University. Doi: 10.27440/d.cnki.gysdu.2022.000017.

Welch, P., 1967. The use of fast Fourier transform for the estimation of power spectra: a method based on time averaging over short, modified periodograms. IEEE Trans. Audio Electroacoust. 15 (2), 70–73. https://doi.org/10.1109/TAU.1967.1161901.

Wen, D., 2014. Study on EEG signal analysis in patients with mild cognitive impairment. Yanshan University. PHD thesis.

Wen, D., Liang, B., Li, J., Wu, L., Wan, X., Dong, X., et al., 2023. Feature extraction method of EEG signals evaluating spatial cognition of community elderly with permutation conditional mutual information common space model. IEEE Trans. Neural Syst. Rehabil. Eng. 31, 2370–2380. https://doi.org/10.1109/TNSRE.2023.3273119.

Wen, D., Bian, Z., Li, Q., Wang, L., Lu, C., Li, X., 2016. Resting-state EEG coupling analysis of amnestic mild cognitive impairment with type 2 diabetes mellitus by using permutation conditional mutual information. Clin. Neurophysiol. 127 (1), 335–348. https://doi.org/10.1016/j.clinph.2015.05.016.

Wen, D., Li, R., Tang, H., Liu, Y., et al., 2022. Task-state EEG signal classification for spatial cognitive evaluation based on multiscale high-density convolutional neural network. IEEE Trans. Neural Syst. Rehabil. Eng. 30, 1041–1051. https://doi.org/10.1109/TNSRE.2022.3166224.

White, D.J., Congedo, M., Ciorciari, J., Silberstein, R.B., 2012. Brain oscillatory activity during spatial navigation: theta and gamma activity link medial temporal and parietal regions. J. Cogn. Neurosci. 24 (3), 686–697. https://doi.org/10.1162/jocn_a_00098.

Zhang, J., Zhang, X., Chen, G., Huang, L., Sun, Y., 2022a. EEG emotion recognition based on cross-frequency granger causality feature extraction and fusion in the left and right hemispheres. Front. Neurosci. 16, 974673. https://doi.org/10.3389/fnins.2022.974673.

Zhang, L., Zhang, R., Guo, Y., Zhao, D., et al., 2022b. Assessing residual motor function in patients with disorders of consciousness by brain network properties of task-state EEG. Cogn. Neurodyn. 16 (3), 609–620. https://doi.org/10.1007/s11571-021-09741-7.